Stabilizing vehicular platoons mixed with regular human-piloted vehicles: an input-to-state string stability approach

Z. ZHAN [a], S.M. WANG [b], T.L. PAN [c], P. CHEN [d], William H.K. LAM [e], R.X. ZHONG [a,*], Y. HAN [a,*]

[a] *School of Intelligent Systems Engineering, Sun Yat-Sen University, Guangzhou, China.*
[b] *Department of Electrical and Computer Engineering, University of Alberta, Alberta, Canada.*
[c] *Research Institute of Smart City, Shenzhen University, Shenzhen, China.*
[d] *School of Transportation Science and Engineering, Beihang University, Beijing, China.*
[e] *Department of Civil and Environmental Engineering, The Hong Kong Polytechnic University, Hong Kong SAR, China*

Abstract

Connected and automated vehicles (CAVs) and regular human-piloted vehicles (RVs) will coexist in the near future. Research has indicated the feasibility of using CAVs to stabilize the traffic flow and eliminate stop-and-go waves. In light of this, we develop nonlinear distributed control schemes to stabilize a mixed vehicular platoon by using a CAV as the leading vehicle. We address several practical challenges such as: the limited information perception capabilities of RVs (e.g., the potential unavailability of the acceleration information of the preceding vehicle for the following vehicle), the uncertainty of the actuators via human drivers or unmodeled dynamics, and external disturbances (e.g., the unavailability of time-varying control input of the leading CAV). Only local information from the preceding vehicle, which can be obtained from commercially implemented adaptive cruise control systems, is known by a following RV, and is thus used in the control design. Platoon control schemes based on the constant space headway policy and constant time headway policy are synthesized. In particular, input-to-state string stability (ISSS) is adopted to aid the control design. Modifications of the ISSS concept are established to cope with the uncertainty and disturbance characteristics while conditions for stability are derived. The proposed control schemes can effectively attenuate or reject the effect of disturbances while maintaining the ISSS property. The relationships between ISSS and other state-of-the-art string stability concepts are clarified. The ISSS concept can include several string stability concepts as special cases. Finally, numerical experiments are conducted to validate the computational feasibility and the effectiveness of the proposed platoon control schemes.

Keywords: Mixed traffic; Vehicular platoon control; External disturbance; Actuator uncertainty; Input-to-state string stability

*Corresponding authors

E-mail addresses: zhanzh3@mail2.sysu.edu.cn (Z. ZHAN)., shimin1@ualberta.ca (S.M. WANG)., glorious9009@gmail.com (T.L. PAN)., cpeng@buaa.edu.cn (P. CHEN)., william.lam@polyu.edu.hk (William H.K. LAM)., zhrenxin@mail.sysu.edu.cn (R.X. ZHONG)., hanyu@mail.sysu.edu.cn (Y. HAN).

1. Introduction

With the rapid development of connected and automated vehicles (CAVs), vehicular platoon control (or cooperative adaptive cruise control (CACC)) for CAVs has become a hot topic since it can simultaneously enhance highway safety and improve traffic efficiency, which are often seen as two contradictory objectives in conventional traffic engineering (Talebpour and Mahmassani, 2016; Besselink and Johansson, 2017; Li et al., 2018; Chen et al., 2019; Khalifa et al., 2020; Pan et al., 2020). The success of CACC relies on the abundance of sensors and machine intelligence equipped by the CAVs and the amount of dedicated short-range communication (DSRC) units, e.g., the vehicle-to-vehicle communication (V2V) and vehicle-to-infrastructure (V2I) communication. Jia and Ngoduy (2016) used the last available state of the leading vehicle to estimate its current state, and designed a consensus-based controller for cooperative driving while considering the impact of intervehicular communication delay and packet loss. Santini et al. (2018) proposed a consensus-based longitudinal controller based on the leader's information obtained from the V2V and V2I communications. Wang et al. (2020a) proposed a CACC strategy for CAVs by incorporating communication-related constraints. Comprehensive reviews on the CACC schemes for CAVs can be found in Feng et al. (2019); Wang et al. (2020); Eskandarian et al. (2019).

However, it is expected that traffic will still be dominated by regular human-piloted vehicles (RVs) in the near future. Compared with CAVs, RVs possess limited information perception capability and permit actuator uncertainty from human drivers. The design of CACC for traffic with a mix of RVs and CAVs remains a major challenge that is critical for the development and deployment of CAVs. Zhang and Orosz (2017) studied the consensus and disturbance attenuation for CACC strategies in a mixed vehicular platoon. Monteil et al. (2019) linearized several car-following models and applied frequency domain stability analysis to derive the string stability of a mixed platoon. Zhou et al. (2020) used multiple CAVs to stabilize a mixed vehicular platoon by using a new definition of "head-to-tail" string stability in the frequency domain. Stern et al. (2018) demonstrated the feasibility of using a CAV to stabilize a mixed traffic flow with RVs and eliminate stop-and-go waves on a ring track. CAVs are usually randomly distributed in the mixed traffic stream in the literature on transportation (see e.g., Xie et al. (2018), Pan et al. (2019), Pan et al. (2020), Zhou et al. (2020)). Jia et al. (2019) found that the order of vehicle types in a heterogeneous platoon of mixed traffic impacts platoon dynamics. It was also found that the scenario of all RVs following the CAVs in the platoon outperforms all other scenarios. On the other hand, adaptive cruise control (ACC) systems are now widely available as standard features for RVs (Gunter et al., 2020). With ACC systems, RVs can detect the relative positions and velocities of the preceding vehicles (Eskandarian et al., 2019). In this paper, ACC systems are considered to be mounted by all RVs. Therefore, it is wise to use a CAV as the leading vehicle of a platoon to control the motions of the following RVs using only the local information that can be accessed by commercially implemented ACC systems. Meanwhile, the trajectory of the CAV can be optimized by the traffic management center (TMC). Several practical challenges must be addressed for the vehicular platoon control of mixed traffic: a) the limited sensing/communication capabilities of RVs (e.g., the acceleration information of the preceding vehicle may not be available to the following vehicle), which means that only local information that can be obtained from commercially implemented ACC systems, such as the relative positions and velocities, should be used in the control schemes; b) the actuator uncertainty due to human drivers and the unmodeled dynamics during the linearization process of the car-following dynamics; and c) external disturbances (e.g., variation in the velocity of the leading vehicle of a platoon and the time-varying control input from the TMC to the leading CAV is unavailable for the following RVs).

A primary objective of vehicular platoon control is string stability. String stability implies that small perturbations will be dissipated (or attenuated) as they propagate along the vehicles in the platoon (Zhou et al., 2019). Otherwise, the platoon is considered string unstable. Platoon string instability can cause the

emergence of traffic jams, such as "stop and go", and it can even cause traffic accidents. The string stability involved in the platoon controller design is interpreted as a performance criterion rather than a stability property in the literature. Therefore, a wide range of notions of string stability have been introduced over the years that are rather ambiguous. Several approaches such as the Lyapunov analysis, spatially invariant linear systems, and the frequency domain criteria have been developed in the literature for analyzing the string stability of a vehicular platoon. In particular, string stability in the literature usually considers a one-vehicle lookahead topology in a homogeneous vehicle platoon of CAVs wherein the response to an initial condition perturbation of a single vehicle in the platoon is considered. This approach ignores the initial condition perturbations of other vehicles and external disturbances. A comprehensive review of these string stability notions can be found in Feng et al. (2019), wherein their relationships are also discussed.

In the field of control theory, the cooperative control problem of vehicles can be modeled as a multi-agent system (MAS) control problem (Cao et al., 2010; Wang et al., 2020b,c). Vehicles that are capable of self-navigation can be viewed as leader agents (the leading vehicles), while other vehicles can be viewed as follower agents (the following vehicles). The desired offset between agents (i.e., formation geometry) that describes the desired distance between any two successive vehicles is another important design criterion in a vehicular platoon control application. Two major policies of formation geometry for vehicular platoons are used in the literature: a) the constant space headway (CSH) policy (Konduri et al., 2017), in which the desired intervehicular distance between two consecutive vehicles is a constant and is independent of the vehicle velocities; and b) the constant time headway (CTH) policy (Bian et al., 2019), wherein the desired intervehicular distance between two consecutive vehicles varies with their vehicle velocities difference. The advantage of the CTH policy is that it can regulate the headway of vehicles according to real-time traffic conditions, e.g., the speed or density of traffic flow. This makes time headway of vehicles more consistent with the reaction time of human drivers. Peng et al. (2014) considered the cooperative tracking of linear multiagent systems with a dynamic leader whose input information is unavailable to any followers. Li et al. (2012) studied the distributed tracking control problem of multiagent systems with general linear dynamics and a leader whose control input is nonzero and not available to any followers. However, these studies did not consider the practical desired distance between neighboring vehicles. To fill this gap, we analyze the CSH policy and CTH policy in the synthesis of the proposed platoon control scheme design. Conditions for stability are provided.

This paper devises vehicular platoon control schemes by using a CAV as the leader to guide the RVs in the platoon. The motion (trajectory, acceleration, or deceleration) of the CAV is planned by the TMC. The time-varying control input to the CAV (from the TMC) is not available to the following RVs. Naturally, the time-varying control input to the CAV is regarded as a bounded disturbance to the vehicular platoon. Each RV adjusts its acceleration and velocity according to the relative motion state of its preceding vehicle. The imperfect actuation of human drivers is considered. Nonlinear platoon control schemes are designed to attenuate the uncertainty and disturbances satisfying certain assumptions. Only local information from the preceding vehicle is known for a following vehicle, i.e., the relative position and velocity, and thus only this limited information is used in the control design. The main contributions of this paper are summarized as follows.

- Vehicular platoon control schemes are proposed for mixed traffic composed of CAVs and RVs considering both the constant space headway (CSH) policy and the constant time headway (CTH) policy.
- The proposed platoon control schemes address several practical challenges regarding the RVs, e.g., the limited sensing/communication capabilities of RVs; the uncertainty of the actuators via human drivers and the unmodeled dynamics during the linearization process of the car following dynamics;

and external disturbances.

- Due to the abovementioned challenges induced by RVs, the concept of input-to-state string stability (ISSS) is introduced for analyzing the string stability of the platoon system. ISSS describes the impact of time-varying unknown bounded external disturbances to the platoon. Assuming the uncertainty is bounded as most existing studies do, the system state is proven to be bounded regardless of the actual uncertainty via the ISSS concept. The relationships between ISSS and other state-of-the-art string stability concepts are clarified. The ISSS concept can include several string stability concepts as special cases.

The rest of this paper is organized as follows. Section 2 formulates the vehicular platoon control problem. Section 3 devises the distributed platoon control schemes with respect to different formation geometry policies. Section 4 analyzes the stability of the proposed control schemes under both the CSH policy and the CTH policy. Section 5 presents numerical experiments. Section 6 concludes the paper. Some preliminaries, useful lemmas and nomenclature are presented in the Appendix.

2. Problem formulation for vehicular platoon control

As summarized by Li et al. (2015), a platoon control system mainly consists of four components: 1) node dynamics; 2) information flow topology; 3) distributed control schemes, and 4) formation geometry. In practical traffic management, managers always need to adjust the real-time velocity and the desired intervehicular distance of the platoon. However, the lack of the V2I communication prevents RVs from receiving real-time control commands. To solve this problem, the CAV is used as the leading vehicle to guide the RVs in the platoon. The leading CAV receives input signals from the TMC through the V2I communication and executes the control commands. The following RVs adjust their accelerations to maintain the same velocities as that of the leading CAV and the desired intervehicular distance by following the distributed platoon control schemes.

2.1. Node dynamics

Consider a platoon of RVs as N following vehicles, indexed by $i = 1, 2, ..., N$, guided by a leading CAV, indexed by $i = 0$, as shown in Fig. 1. Use $\mathcal{V} = \{1, 2, \cdots, N\}$ and $\bar{\mathcal{V}} = \{0, 1, 2, \cdots, N\}$ to represent the set of the following vehicles and all vehicles, respectively.

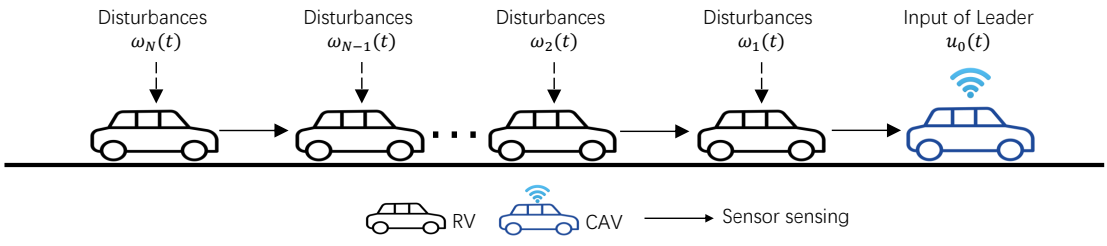

Fig. 1. Platoon of RVs following the leading CAV

Let n denote the dimension of research objects, $p_i(t) \in \mathbb{R}^n$ and $v_i(t) \in \mathbb{R}^n$ represent the positions and velocities of vehicles respectively. Then $d_i(t) = p_i(t) - p_{i-1}(t)$ denote the position difference between vehicle i and vehicle $i-1$.

In the platoon control problem, the formation geometry, which describes the desired distance between any two successive vehicles, is another important design criterion. The control objective is to regulate the motions of RVs, such that all RVs can drive with a desired intervehicular distance while maintaining the same velocity as that of the leading CAV.

Two major policies of formation geometry for vehicular platoons are used in the literature: a) the CSH policy (Konduri et al., 2017), and b) the CTH policy (Bian et al., 2019). Using $d^*_{i,i-1}(t) \in \mathbb{R}^n$ to represent the desired intervehicular distance between two consecutive vehicles. For the CSH policy, the desired intervehicular distance between two consecutive vehicles is independent of the vehicle velocities. The CSH policy can be formulated as

$$d^*_{i,i-1}(t) = s_i \tag{1}$$

where $s_i \in \mathbb{R}^n$ is a constant vector that represents the desired standstill distance between vehicle i and vehicle $i-1$.

For the CTH policy, the desired intervehicular distance between two consecutive vehicles varies with their velocity differences $\Delta v_i(t)$. For the sake of simplicity, the values of the desired time headway τ_i are assumed to be the same for all vehicles, i.e., $\tau_i = \tau$ for all $i \in \mathcal{V}$. The CTH policy can be formulated as:

$$d^*_{i,i-1}(t) = \tau \Delta v_i(t) + s_i \tag{2}$$

where $\tau = diag\{\tau_1, \tau_2, \cdots, \tau_n\} \in \mathbb{R}^{n\times n}$ is a diagonal matrix that represents the desired time headway of vehicles, and $s_i \in \mathbb{R}^n$ possess the same meaning as in the CSH policy (1).

Then the position deviation $\Delta d_i(t)$ from $d^*_{i,i-1}(t)$ and the speed difference $\Delta v_i(t)$ with respect to the preceding vehicle can be defined as:

$$\Delta d_i(t) = p_i(t) + d^*_{i,i-1}(t) - p_{i-1}(t) = d^*_{i,i-1}(t) + d_i(t) \tag{3}$$

$$\Delta v_i(t) = v_i(t) - v_{i-1}(t) \tag{4}$$

Node dynamics describes the behavior of each involved vehicle. For RVs equipped with ACC systems, the control commands can be executed by the control unit of the ACC system. However, due to the actuator uncertainty from human drivers and the unmodeled dynamics during the linearization process of the car following dynamics, disturbances should be considered. By using disturbance $\omega_i(t)$ to model the inaccurate actuation by human drivers, a linear second-order model (Li et al., 2018; Zegers et al., 2017; Li et al., 2011; Liu and Su, 2019) can be used to describe the vehicular dynamics (for $i \in \bar{\mathcal{V}}$):

$$\begin{aligned} \dot{p}_i(t) &= v_i(t), \\ \dot{v}_i(t) &= u_i(t) + \omega_i(t) \end{aligned} \tag{5}$$

where $u_i(t) \in \mathbb{R}^n$ ($i \in \mathcal{V}$) represents the control input of vehicle i. $\omega_i(t) \in \mathbb{R}^n$ represents the disturbances acting on the dynamics of the following vehicle i ($\omega_0(t) = 0$), which are induced by the uncertainty present in the actuator dynamics (inaccurate operation by human drivers) and the unmodeled RV car-following dynamics (induced by the linearization process of the dynamics).

It should be noted $u_0(t)$ is the reference input control signal of the leading CAV obtained from the TMC, which is unknown to the following RVs. This signal is thus regarded as an external disturbance to the platoon system. And the design of $u_0(t)$ for the leading CAV is not a considered topic, instead, the design

of the control schemes $u_i(t)$ ($i \in \mathcal{V}$) for the following RVs is the interest of this paper.

For the CTH policy, the objective of platoon control is to regulate

$$\begin{aligned}\Delta\dot{d}_i(t) &= \Delta v_i(t) + \tau(u_i(t) + \omega_i(t) - u_{i-1}(t) - \omega_{i-1}(t)),\\ \Delta\dot{v}_i(t) &= u_i(t) + \omega_i(t) - u_{i-1}(t) - \omega_{i-1}(t)\end{aligned} \tag{6}$$

Define $x_i(t) = [\Delta d_i(t), \Delta v_i(t)]^T \in \mathbb{R}^{2n}$ as the tracking deviation between vehicle i and vehicle $i-1$, the dynamics of the leading CAV and the following RVs can be formulated in a state-space form as follows (for $i \in \mathcal{V} = \{1, 2, ..., N\}$):

$$\dot{x}_i(t) = Ax_i(t) + (B+E)[u_i(t) + \omega_i(t)] - (B+E)[u_{i-1}(t) + \omega_{i-1}(t)] \tag{7}$$

$A = \begin{bmatrix} 0 & 1 \\ 0 & 0 \end{bmatrix} \otimes I_n$, $B = \begin{bmatrix} 0 \\ 1 \end{bmatrix} \otimes I_n$, $E = \begin{bmatrix} \tau \\ 0 \end{bmatrix}$.

It should be noted that the CSH policy (1) can be viewed as a special case of the CTH policy by letting $\tau = \mathbf{0}$ in (2). Thus the remained paper mainly analyses the CTH policy, and the CSH policy can be analysed as the CTH policy by letting $\tau = \mathbf{0}$, i.e., $E = \mathbf{0}$, in (7).

Note that the dimension n means that the discussed controller can be applied in different dimensions of space. For example, the conventional vehicular platoon control in the longitudinal dimension can be described by letting $n = 1$ (i.e., 1-dimensional case) in (5).

Besides, in many applications, such as the platoon control of vehicles along a curved road or across an intersection, the coordinated control of a group of mobile robots and the formation control of unmanned aerial vehicles, multiple dimensional motions must be regulated. A similar analysis of the higher dimensional case of (5) can be performed by using the Kronecker product. For example, in some scenarios we need to control the vehicular dynamics in both longitudinal and lateral dimension, i.e., $n = 2$, the 2-dimensional case. Vehicular platoon control on a curved road and passing through an intersection belong to this case. For the 2-dimensional case, while disturbance $\omega_i(t)$ is induced by the actuator uncertainty from human drivers, the dynamics of the leading CAV and following RVs can be described as ($i \in \bar{\mathcal{V}}$):

$$\begin{aligned}\dot{p}_{xi}(t) &= v_{xi}(t),\\ \dot{p}_{yi}(t) &= v_{yi}(t),\\ \dot{v}_{xi}(t) &= u_{xi}(t) + \omega_{xi}(t),\\ \dot{v}_{yi}(t) &= u_{yi}(t) + \omega_{yi}(t)\end{aligned} \tag{8}$$

The dynamics (8) can also be reformulated in a state-space form as in (7) by defining the corresponding state $x_i(t) = [\Delta d_i^T(t), \Delta v_i^T(t)]^T = [\Delta d_{xi}(t), \Delta d_{yi}(t), \Delta v_{xi}(t), \Delta v_{yi}(t)]^T$, where $\Delta d_{xi}(t)$ and $\Delta d_{yi}(t)$ represent the longitudinal and lateral position deviations of vehicle i, respectively, $\Delta v_{xi}(t)$ and $\Delta v_{yi}(t)$ are the longitudinal and lateral velocities of vehicle i, respectively. The control input $u_i(t) = [u_{xi}(t), u_{yi}(t)]^T$, the disturbance $\omega_i(t) = [\omega_{xi}(t), \omega_{yi}(t)]^T$, matrix $A = \begin{bmatrix} 0 & 1 \\ 0 & 0 \end{bmatrix} \otimes I_2$, and $B = \begin{bmatrix} 0 \\ 1 \end{bmatrix} \otimes I_2$, and $\tau = diag\{\tau_1, \tau_2\}$ represent the the longitudinal and lateral desired time headway of vehicles. In Example 5.2, we simulate the vehicular platoon control for a curved road case via the proposed control schemes.

Remark 2.1. It should be noted that (5), (7) and (8) represent the single platoon control case. Multiplatoon

control can be achieved by applying our control schemes in every platoon, while the cooperation between the leading CAV of the platoons can be achieved by refining the network communication. A multiplatoon control case is simulated in Example 5.3 as an important application of our control schemes.

Assumption 2.1. The reference input control signal $u_0(t)$ of the leading CAV in (7) is bounded, i.e., $\|u_0(t)\| \leq r_1$, where r_1 is the control input bound of the leading CAV. The disturbances $\omega_i(t)$ are bounded for all following RVs, i.e., $\|\omega_i(t)\| \leq r_2$ for all .

In particular, the reference input control signal of the leading CAV obtained from the TMC and the disturbances acting on the dynamics of the following RVs in practical scenarios are always bounded due to the mechanical characteristics. Thus, Assumption 2.1 is reasonable.

2.2. Information flow topology

Information flow topology defines how vehicles exchange information with each other and thus describes the information that can be used by local control schemes. In this paper, RVs are assumed to be equipped with commercially implemented ACC systems, which is consistent with the tendencies of the automotive industry (Gunter et al., 2020). There are no V2V and V2I communications for RVs. Thus, the accelerations of all vehicles and all information about other vehicles beyond those in the neighborhood cannot be obtained. Each RV can only receive the relative position and velocity from its preceding vehicle by the microwave radar of the ACC system.

A network of systems consisting of N following vehicles, indexed by $i \in \mathcal{V} = \{1, 2, \cdots, N\}$ is considered. Each following vehicle is considered as a node. Then the neighboring relationship among the following vehicles can be described by a graph $\mathcal{G} = \{\mathcal{V}, \mathcal{E}, \mathcal{A}\}$, whose edge set is $\mathcal{E} \subseteq \mathcal{V} \times \mathcal{V}$ and where an element (i, j) describes the communication from a following vehicle i to another following vehicle j. The neighbor vehicle set of vehicle i is denoted by $\mathcal{A}_i = \{j \mid (j, i) \in \mathcal{E}\}$. $\mathcal{A} = \left[a_{ij}\right]_{i,j=1}^{N} \in \mathbb{R}^{N\times N}$ is used to denote the adjacent matrix of graph $\mathcal{G}$, where a_{ij} is the weight of edge (j, i) with $a_{ij} = 1$ if $(i, j) \in \mathcal{E}$ (i.e., if a following vehicle i can obtain information from a following vehicle j) and $a_{ij} = 0$ otherwise. A degree matrix is defined as a diagonal matrix $\mathcal{D} = diag\{d_1, d_2, \cdots, d_N\} \in \mathbb{R}^{N\times N}$ with $d_i = \sum_{j\in\mathcal{A}_i} a_{ij}$ for node i. The Laplacian matrix associated with the graph $\mathcal{G}$ is defined as $\mathcal{L} = \mathcal{D} - \mathcal{A}$. Based on the sensing characteristics of the ACC system, information flow topology is equivalent to predecessor following (PF) topology (Xiao and Gao, 2011). According to the sensing topology described in Fig. 1, the neighborhood matrix for the following RVs and the corresponding Laplace matrix can be written as:

$$\mathcal{A} = \begin{bmatrix} 0 & 0 & \cdots & 0 & 0 \\ 1 & 0 & \cdots & 0 & 0 \\ 0 & 1 & \cdots & 0 & 0 \\ \vdots & \vdots & \ddots & \vdots & \vdots \\ 0 & 0 & \cdots & 1 & 0 \end{bmatrix} \quad \mathcal{L} = \begin{bmatrix} 0 & 0 & 0 & \cdots & 0 \\ -1 & 1 & 0 & \cdots & 0 \\ 0 & -1 & 1 & \cdots & 0 \\ \vdots & \vdots & \ddots & \ddots & \vdots \\ 0 & 0 & \cdots & -1 & 1 \end{bmatrix} \tag{9}$$

where $\mathcal{L}$ represents the link between the following RVs.

To represent the link between the following vehicles and the leading vehicle, a leader adjacency matrix is defined as $\mathcal{A}_0 = diag\{a_{10}, a_{20}, \cdots, a_{N0}\}$, where $a_{i0} = 1$ if and only if a following vehicle i can access information about the leading vehicle; otherwise, $a_{i0} = 0$. In the platoon system of this paper, only the RV

following directly behind the leading CAV, i.e., the following vehicle $i = 1$, can obtain the relative position and velocity of the leading CAV, thus $\mathcal{A}_0 = diag\{1, 0, 0, \cdots, 0\}$. Let $H = \mathcal{L} + \mathcal{A}_0$ represent the relationship between the following vehicles and other following vehicles as well as the leading vehicle, then:

$$H = \begin{bmatrix} 1 & 0 & 0 & \cdots & 0 \\ -1 & 1 & 0 & \cdots & 0 \\ 0 & -1 & 1 & \cdots & 0 \\ \vdots & \vdots & \ddots & \ddots & \vdots \\ 0 & 0 & \cdots & -1 & 1 \end{bmatrix} \tag{10}$$

3. Control scheme design

It is assumed that all RVs are equipped with commercially implemented ACC systems. Based on the ACC systems, the available information for control schemes for RVs is analyzed in Subsection 3.1, and the control schemes are designed in Subsection 3.2 according to the available information.

3.1. Available information for the control schemes

This subsection analyzes the available information for the control schemes of the platoon system in this paper. As described in Section 2, characteristics for the designs of the control schemes can be stated as follows:

- RVs can only obtain local relative information, i.e., the relative positions and velocities of the preceding vehicle, from the microwave radars of their commercially implemented ACC systems.
- RVs do not possess the ability to communicate by V2V or V2I communication, and only the RV following directly behind the leading CAV can obtain the relative position and velocity of the leading CAV.
- The time-varying control input of the leading CAV and the disturbances acting on the following RVs are unavailable to any of the RVs.

Based on the available information, the control schemes can be designed as described in the next subsection.

3.2. Control scheme design according to the available information

To make the control schemes practical for application, for vehicle i, the relative positions $\Delta d_i(t)$ and relative velocities $\Delta v_i(t)$ of the preceding vehicle as well as its own information can be used. The state deviation with respect to the preceding vehicle $x_i(t) = [\Delta d_i(t), \Delta v_i(t)]^T \in \mathbb{R}^{2n}$ can be considered to use in the control schemes.

Based on the relative position and velocity of the preceding vehicle, inspired by the results in Peng et al. (2014) and Li et al. (2012), the following control schemes (for $i \in \mathcal{V}$) can be proposed for each following

RV:

$$u_i(t) = c_1 K x_i(t) + c_2 g\left(x_i(t)\right) \tag{11}$$

where $c_1 > 0$ and $c_2 > 0$ are constant gains and K is feedback gain matrix. $g(\cdot)$ is a nonlinear function that is used to eliminate the impact of the time-varying reference input signal $u_0(t)$ on the dynamics of the following RVs. $g(\cdot)$ is defined as follows:

$$g(x_i(t)) = \begin{cases} \dfrac{K x_i(t)}{\|K x_i(t)\|}, & if \quad K x_i(t) \neq 0 \\ 0, & if \quad K x_i(t) = 0 \end{cases} \tag{12}$$

Remark 3.1. It should be noted that the control schemes (11) of the following RVs only utilize the relative positions and velocities of the preceding vehicle and the state information (positions and velocities) of the specific RV itself. Usually, RVs can obtain these information by using the radar of the ACC system, GPS and velocity sensors. Thus, (11) is fully distributed and practically applicable for RVs.

4. Stability analysis of the closed-loop system

This section first recalls commonly used definitions of string stability in the platoon control problem. To cope with the time-varying unknown bounded external input $u_0(t)$ and disturbance $\omega_i(t)$ acting on the dynamics of the following RVs, ISSS recommended by Feng et al. (2019) is adopted to aid the control scheme design. After the clarification of the relationships between ISSS and other state-of-the-art string stability concepts, the ISSS concept can be concluded to include several string stability concepts as special cases. Then, stability conditions for platoon control schemes that synthesize the CSH policy and CTH policy are derived.

4.1. Various platoon stability definitions and their relations

The tracking deviation (for $i \in \mathcal{V}$) from the desired state with respect to the leading CAV, i.e., the tracking deviation between vehicle i and the leading CAV, $\eta_i(t) \in \mathbb{R}^{2n}$ is defined as:

$$\eta_i(t) = \begin{bmatrix} p_i(t) + \sum_{j=1}^{i} d^*_{j,j-1}(t) - p_0(t) \\ v_i(t) - v_0(t) \end{bmatrix} \tag{13}$$

For heterogeneous platoon, Jia and Ngoduy (2016) and Jia et al. (2019) proposed the following platoon stability concept from consensus perspective as follows:

Definition 4.1. (Jia and Ngoduy, 2016; Jia et al., 2019) (Platoon stability). Given the system in (7), if the state of any following vehicle $i \in \mathcal{V}$ within the same platoon satisfies:

$$\lim_{t\to\infty} \|\eta_i(t)\| \leq C_0, \tag{14}$$

where C_0 is the upper bound of the constant positive state deviation, then the platoon is said to reach the platoon stability.

$\mathcal{L}_p$ string stability (LPSS) was proposed by Ploeg et al. (2013) to explicitly handle the external input for the leading vehicle. For the following cascaded state-space system:

$$\begin{aligned} \dot{x}_0 &= f_r(x_0, u_0) \\ \dot{x}_i &= f_i(x_i, x_{i-1}) \\ y_i &= h(x_i) \end{aligned} \tag{15}$$

where u_0 is the external input of the leading vehicle, x_i is the state for $i \in \bar{\mathcal{V}}$, and y_i is the output signal.

Definition 4.2. (Ploeg et al., 2013; Feng et al., 2019) (LPSS) The equilibrium point $x_i = 0,\ i \in \bar{\mathcal{V}}$ of system (15) is LPSS if there exist class $\mathcal{K}$ functions α and β such that, for any initial state $x(0)$, where $x = (x_0, \cdots, x_N)$ is the state vector, any external input for the leading vehicle u_0, satisfies:

$$\sup_i \|y_i(t)\|_{\mathcal{L}_p} \leq \alpha\left(\|u_0(t)\|_{\mathcal{L}_p}\right) + \beta\left(\|x(0)\|_p\right) \tag{16}$$

The concept of disturbance string stability (DSS) was proposed by Besselink and Johansson (2017) to extend these definitions to systems with external disturbances for all vehicles with zero initial condition perturbations.

Definition 4.3. (Besselink and Johansson, 2017) (DSS) The equilibrium point $x_i = 0,\ i \in \bar{\mathcal{V}}$ of a system is DSS if there exist a class $\mathcal{K}$ function α, a class $\mathcal{KL}$ function γ, and constants $k_1,\ k_2 \in \mathcal{R}^+$, such that for any initial condition $x_i(0)$ and additive disturbance $\omega_i(t),\ i \in \bar{\mathcal{V}}$, satisfying

$$\sup_i |x_i(0)| < k_1, \sup_i \|\omega_i(t)\|_\infty < k_2 \tag{17}$$

the solution $x_i(t),\ i \in \bar{\mathcal{V}}$, exists for all $t \geq 0$ and satisfies

$$\sup_i |x_i(t)| \leq \gamma\left(\sup_i |x_i(0)|, t\right) + \alpha\left(\sup_i \|\omega_i\|_\infty^{[0,t]}\right) \tag{18}$$

ISSS was recommended by Feng et al. (2019) as the formal definition of vehicle platoon string stability. ISSS characterizes the boundedness of state fluctuations and the convergence of state fluctuations caused by initial condition deviations, where boundedness and convergence hold for any platoon length. ISSS means that bounded inputs (external disturbances) generate bounded states.

Definition 4.4. (Feng et al., 2019) (ISSS) The platoon system (7) is said to be ISSS if there exist a class $\mathcal{K}$ function α and a class $\mathcal{KL}$ function γ such that, for each initial condition deviation $x(0)$ and each input $u(t)$, satisfying:

$$\|x(0)\|_p < k_1, \|u\|_{\mathcal{L}_\infty}^{[0,t]} < k_2 \tag{19}$$

there exists:

$$\begin{aligned} \|x(t)\|_p \leq \gamma(\|x(0)\|_p, t) + \alpha(\|u\|_{\mathcal{L}_\infty}^{[0,t]}) \\ \forall t \geq 0 \end{aligned} \tag{20}$$

Input-to-state stability (ISS) proposed in the field of control theory is a formal mathematical tool for analyzing the ISSS. Details of ISS can be found in (Sontag and Wang, 1995; Sontag, 2008).

Definition 4.5. (Sontag and Wang, 1995; Sontag, 2008) A smooth function $V : \mathbb{R}^\rho \to \mathbb{R}$ is called an ISS-Lyapunov function for the system (7) if there exist class $\mathcal{K}_\infty$ functions $\alpha_1, \alpha_2, \alpha_3, \alpha_4$, such that:

$$\alpha_1(\|x\|) \leq V(x) \leq \alpha_2(\|x\|) \tag{21}$$

for any $x \in \mathbb{R}^\rho$ and

$$\dot{V}(x) \leq -\alpha_3(\|x\|) + \alpha_4(\|u\|) \tag{22}$$

for any $x \in \mathbb{R}^\rho$ and any $u \in \mathbb{R}^m$.

Lemma 4.1. (Sontag and Wang, 1995; Sontag, 2008) A system is ISS if and only if it results in a smooth ISS-Lyapunov function.

According to Definition 4.5 and Lemma 4.1 for ISS, a platoon system is ISSS if and only if there exists a smooth ISS-Lyapunov function.

According to the definition above of string stability, the following equivalences hold:

$$\begin{aligned} &(1) \quad ISSS \quad \Longrightarrow \quad LPSS \\ &(2) \quad ISSS \quad \overset{p=\infty}{\Longrightarrow} \quad DSS \\ &(3) \quad ISSS \quad \overset{p=2}{\Longrightarrow} \quad platoon\ stability \end{aligned} \tag{23}$$

where the proofs of (1) and (2) were given by Feng et al. (2019), and the proof of (3) is given as follows:

Proof: ISSS $\Longrightarrow$ platoon stability: If a system is ISSS, letting $p = 2$, we obtain

$$\|x(t)\| \leq \gamma(\|x(0)\|, t) + \alpha(\|u\|_\infty) \tag{24}$$

Thus,

$$\lim_{t\to\infty} \|x(t)\| = \alpha(\|u\|_\infty) \leq \alpha(k_2) \tag{25}$$

According to (13), it should be noted that:

$$x_i(t) = \eta_i(t) - \eta_{i-1}(t) \tag{26}$$

By letting $\eta(t) = [\eta_1^T(t), \eta_2^T(t), \cdots, \eta_N^T(t)]^T$, and $x(t) = [x_1^T(t), x_2^T(t), \cdots, x_N^T(t)]^T$, (26) can be rewritten in a compact form as:

$$x(t) = (H \otimes I_{2n})\, \eta(t) \tag{27}$$

where the tracking deviations of the leading CAV η_0 and x_0 are defined as $\eta_0 = 0$ and $x_0 = 0$. Therefore, we obtain:

$$\lim_{t\to\infty} \|\eta(t)\| \leq \left\|(H \otimes I_{2n})^{-1}\right\| \alpha(k_2) \tag{28}$$

Thus the conclusion follows.

As concluded above, ISSS can describe the impact of time-varying unknown bounded external disturbances on the platoon, and ISSS can include the platoon stability concepts described in Definition 4.1, Definition 4.2, and Definition 4.3 as special cases. Therefore, ISSS is adopted to aid the control scheme design and analyze the string stability of the platoon system in this paper.

4.2. Stability analysis with the CTH policy and the CSH policy

This subsection analyzes the stability of the platoon control scheme based on the CTH policy and the CSH policy. As the CSH policy is a special case of CTH policy, the subsection only gives the proof of the CTH policy Theorem 4.1, and the proof of the CSH policy can be obtained by letting $\tau = 0$ (i.e.,$E = 0$).

According to (7) and the control schemes proposed in (11), we obtain the closed-loop dynamics of the tracking deviations as ($i = 2, 3, \cdots, N$):

$$\begin{aligned}\dot{x}_i(t) =& Ax_i(t) + c_1(B+E)K[x_i(t) - x_{i-1}(t)] \\ &+ c_2(B+E)[g(x_i(t)) - g(x_{i-1}(t))] \\ &+ (B+E)[\omega_i(t) - \omega_{i-1}(t)]\end{aligned} \tag{29}$$

For vehicle $i = 1$, the closed-loop network dynamics of the tracking deviations can be written as:

$$\begin{aligned}\dot{x}_1(t) =& Ax_1(t) + c_1(B+E)Kx_1(t) + c_2(B+E)g(x_1(t)) \\ &+ (B+E)\omega_1(t) - (B+E)u_0(t)\end{aligned} \tag{30}$$

Then, (29) and (30) can be rewritten in a compact form as:

$$\begin{aligned}\dot{x}(t) =& (I_N \otimes A + c_1 H \otimes (B+E)K]\, x(t) \\ &+ c_2[H \otimes (B+E)]\, G(x) + H \otimes (B+E)\,\omega(t) \\ &- [\mathcal{A}_0 \mathbf{1} \otimes (B+E)]\, u_0(t)\end{aligned} \tag{31}$$

where $\omega(t) = [\omega_1^T(t), \omega_2^T(t), \cdots, \omega_N^T(t)]^T$, $G(x) = [g^T(x_1(t)), g^T(x_2(t)), \cdots, g^T(x_N(t))]^T$.
Then, Theorem 4.1 holds for the CTH policy as follows:

Theorem 4.1. Under the CTH policy, the ISSS of the platoon system is achieved when the parameters of the platoon control schemes (11) are designed with the requirements that $c_2 \geq 0$, $K = -(B+E)^T P$, while c_1 and the positive definite matrix P are the solutions to the following matrix inequality:

$$A^T P + PA + 2P(B+E)(B+E)^T P - c_1 \lambda_{min}(\Sigma) P(B+E)(B+E)^T P < 0 \tag{32}$$

where $\lambda_{min}(\Sigma)$ is the minimum eigenvalue of $\Sigma = H^T + H$.

When $c_2 \geq r_1$, the impact of the time-varying external disturbance $u_0(t)$ can be fully eliminated, and (32) can be reduced to:

$$A^T P + PA + P(B+E)(B+E)^T P - c_1 \lambda_{min}(\Sigma) P(B+E)(B+E)^T P < 0 \tag{33}$$

Proof 4.1. Consider the Lyapunov function candidate (34) (Lyashevskiy and Meyer, 1995) to analyze the stability of the system under the CTH policy:

$$V = x^T(t)(I_N \otimes P)x(t) \tag{34}$$

P is positive definite, thus V is positive definite. Let $K = -(B+E)^T P$, the time derivative of V along the trajectory of (31) is given by:

$$\begin{aligned}\dot{V} =& \dot{x}^T(t)(I_N \otimes P)x(t) + x^T(t)(I_N \otimes P)\dot{x}(t)\\ =& x^T(t)\left[I_N \otimes (A^T P + PA) - c_1\Sigma \otimes P(B+E)(B+E)^T P\right]x(t)\\ &+ 2c_2 x^T(t)[H \otimes P^T(B+E)]G(x) - 2x^T(t)\left[\mathcal{A}_0\mathbf{1} \otimes P^T(B+E)\right]u_0(t)\\ &+ 2x^T(t)[H \otimes P^T(B+E)]\omega(t)\end{aligned} \tag{35}$$

where $\Sigma = H^T + H$ is positive definite.

By using $\mathcal{A}_0 = diag\{a_{10}, a_{20}, \cdots, a_{N0}\}$, we obtain:

$$\begin{aligned}&- 2x^T(t)\left[\mathcal{A}_0\mathbf{1} \otimes P^T(B+E)\right]u_0(t)\\ =& -2\sum_{i=1}^{N} x_i^T P^T(B+E)a_{i0}u_0(t)\\ \leq& 2\sum_{i=1}^{N} a_{i0}\|(B+E)^T P x_i\|\|u_0(t)\|_\infty\\ \leq& 2r_1\sum_{i=1}^{N} a_{i0}\|(B+E)^T P x_i\|\end{aligned} \tag{36}$$

From Young's Inequality:

$$\begin{aligned}&2x^T(t)[H \otimes P^T(B+E)]\omega(t)\\ \leq& x^T(t)\left(I_N \otimes P(B+E)(B+E)^T P\right)x(t) + \lambda^2(H)_{max}\|\omega(t)\|^2\end{aligned} \tag{37}$$

Noting that:

$$\begin{aligned}&x_i^T P^T(B+E)g(x_i) = -\left\|(B+E)^T P x_i\right\|\\ &-x_i^T P^T(B+E)g\left(x_j\right) \leq \left\|x_i^T P^T(B+E)\right\|\left\|g\left(x_j\right)\right\| \leq \left\|(B+E)^T P x_i\right\|\end{aligned} \tag{38}$$

Thus $x_i^T P^T(B+E)[g(x_i)-g(x_j)] \leq -\left\|(B+E)^T P x_i\right\| + \left\|(B+E)^T P x_i\right\| = 0$. Then:

$$
\begin{aligned}
&2c_2 x^T(t)\left[H \otimes P^T(B+E)\right] G(x) \\
=&2c_2 \sum_{i=1}^{N} x_i^T P^T(B+E) \sum_{j=0}^{N} a_{ij}\left(g(x_i)-g\left(x_j\right)\right) \\
=&2c_2 \sum_{i=1}^{N} x_i^T P^T(B+E)\left[a_{i0}(g(x_i)-g(x_0))+a_{i1}(g(x_i)-g(x_1))+\cdots+a_{iN}(g(x_i)-g(x_N))\right] \\
\leq&-2c_2 \sum_{i=1}^{N} a_{i0}\left\|(B+E)^T P x_i\right\|
\end{aligned} \tag{39}
$$

When $c_2 \geq r_1$, choose c_1 and a positive definite matrix P such that $A^T P + PA + P(B+E)(B+E)^T P - c_1\lambda_{min}(\Sigma)P(B+E)(B+E)^T P = -Q < 0$, where Q is positive definite. Let M be a unitary matrix such that $M^T \Sigma M = diag\{\sigma_1, \sigma_2, \cdots, \sigma_N\}$, where σ_i is the eigenvalue of Σ. Let $\lambda_{min}(\Sigma)$ denote the minimum eigenvalue of Σ. We introduce a state transformation $\epsilon(t) = (M^T \otimes I_{2n})x(t)$ with $\epsilon(t) = [\epsilon_1^T(t), \epsilon_2^T(t), \cdots, \epsilon_N^T(t)]^T$. Thus:

$$
\begin{aligned}
\dot{V} \leq& x^T(t)\left[I_N \otimes (A^T P + PA) - c_1\Sigma \otimes P(B+E)(B+E)^T P\right] x(t) + 2(r_1 - c_2)\sum_{i=1}^{N} a_{i0}\|(B+E)^T P x_i\| \\
&+ x^T(t)\left(I_N \otimes P(B+E)(B+E)^T P\right) x(t) + \lambda_{max}^2(H)\|\omega(t)\|^2 \\
\leq& x^T(t)\left[I_N \otimes (A^T P + PA) - c_1\Sigma \otimes P(B+E)(B+E)^T P + I_N \otimes P(B+E)(B+E)^T P\right] x(t) \\
&+ \lambda_{max}^2(H)\|\omega(t)\|^2 \\
\leq& \sum_{i=1}^{N} \epsilon_i^T\left[A^T P + PA + P(B+E)(B+E)^T P - c_1\sigma_i P(B+E)(B+E)^T P\right]\epsilon_i + \lambda_{max}^2(H)\|\omega(t)\|^2 \\
\leq& \sum_{i=1}^{N} \epsilon_i^T\left[A^T P + PA + P(B+E)(B+E)^T P - c_1\lambda_{min}(\Sigma)P(B+E)(B+E)^T P\right]\epsilon_i \\
&+ \lambda_{max}^2(H)\|\omega(t)\|^2 \\
=& -\sum_{i=1}^{N} \epsilon_i^T Q \epsilon_i + \lambda_{max}^2(H)\|\omega(t)\|^2 \\
\leq& -\lambda_{min}(Q)\|x(t)\|^2 + \lambda_{max}^2(H)\|\omega(t)\|^2
\end{aligned} \tag{40}
$$

For the case in which $c_2 \geq r_1$, the impact of the time-varying input (external disturbance) $u_0(t)$ can be fully eliminated by (12). According to Definition 4.5, it is clear that (34) is an ISS-Lyapunov function, and thus, the vehicular platoon system with the CTH policy is ISSS according to Lemma 4.1.

When $0 < c_2 < r_1$, the existence of c_2 can weaken, rather than fully eliminate, the impact of the time-varying input (external disturbance) $u_0(t)$. Assume that $c_2 = \kappa_1 r_1$ and $\|u_0(t)\| = \kappa_2(t) r_1$, where $\kappa_1 \in (0,1)$

and $\kappa_2(t) \in (0, 1]$. Let $\kappa(t) = 1 - \frac{\kappa_1}{\kappa_2(t)} < 1$. Then:

$$\begin{aligned} \|u_0(t)\| - c_2 =& \|u_0(t)\| - \frac{\kappa_1}{\kappa_2(t)}\|u_0(t)\| \\ =& \kappa(t)\|u_0(t)\| \end{aligned} \tag{41}$$

Choose c_1 and a positive definite matrix P such that $A^T P + PA + 2P(B+E)(B+E)^T P - c_1\lambda_{min}(\Sigma)P(B+E)(B+E)^T P = -Q < 0$, where Q is positive definite. Similar to the analysis in (40), using (41), we obtain:

$$\begin{aligned} \dot{V} \leq& x^T(t)\left[I_N \otimes (A^T P + PA) - c_1\Sigma \otimes P(B+E)(B+E)^T P\right] x(t) \\ &+ 2(r_1 - c_2)\sum_{i=1}^{N} a_{i0}\|(B+E)^T P x_i\| + x^T(t)(I_N \otimes P(B+E)(B+E)^T P)x(t) + \lambda_{max}^2(H)\|\omega(t)\|^2 \\ \leq& x^T(t)\left[I_N \otimes (A^T P + PA) - c_1\Sigma \otimes P(B+E)(B+E)^T P + I_N \otimes (P(B+E)(B+E)^T P)\right] x(t) \\ &+ 2\kappa(t)\|u_0(t)\|\sum_{i=1}^{N} a_{i0}\|(B+E)^T P x_i\| + \lambda_{max}^2(H)\|\omega(t)\|^2 \\ \leq& x^T(t)\left[I_N \otimes (A^T P + PA) - c_1\Sigma \otimes P(B+E)(B+E)^T P + I_N \otimes (P(B+E)(B+E)^T P)\right] x(t) \\ &+ \sum_{i=1}^{N}\|(B+E)^T P\xi_i\|^2 + \kappa^2(t)\|u_0(t)\|^2 + \lambda_{max}^2(H)\|\omega(t)\|^2 \\ \leq& \sum_{i=1}^{N}\epsilon_i^T\left[A^T P + PA + 2P(B+E)(B+E)^T P - c_1\sigma_i P(B+E)(B+E)^T P\right]\epsilon_i \\ &+ \kappa^2(t)\|u_0(t)\|^2 + \lambda_{max}^2(H)\|\omega(t)\|^2 \\ =& -\sum_{i=1}^{N}\epsilon_i^T Q\epsilon_i + \kappa^2(t)\|u_0(t)\|^2 + \lambda_{max}^2(H)\|\omega(t)\|^2 \\ \leq& -\lambda_{min}(Q)\|x(t)\|^2 + \kappa^2(t)\|u_0(t)\|^2 + \lambda_{max}^2(H)\|\omega(t)\|^2 \end{aligned} \tag{42}$$

According to Definition 4.5, it is clear that (34) is an ISS-Lyapunov function where:

$$\begin{aligned} \alpha_1(\|x\|) &= \lambda_{min}(I_N \otimes P)\|x\|^2 \\ \alpha_2(\|x\|) &= \lambda_{max}(I_N \otimes P)\|x\|^2 \\ \alpha_3(\|x\|) &= \lambda_{min}(Q)\|x\|^2 \\ \alpha_4(\|u\|) &= \kappa^2(t)\|u_0(t)\|^2 + \lambda_{max}^2(H)\|\omega(t)\|^2 \end{aligned} \tag{43}$$

Thus, the vehicular platoon system is ISSS according to Lemma 4.1. Platoon stability Definition 4.1, and other vehicle platoon string stability Definition 4.2, and Definition 4.3 are achieved naturally. ∎

Similarly, by letting $E = 0$, ISSS conditions of the CSH policy can be shown as follows.

Theorem 4.2. Under the CSH policy, the ISSS of the vehicular platoon system is achieved when the parameters of the platoon control schemes (11) are designed with the requirements that $c_2 \geq 0$, $K = -B^T P$,

while c_1 and the positive definite matrix P are the solutions to the following matrix inequality:

$$A^T P + PA + 2PBB^T P - c_1 \lambda_{min}(\Sigma) PBB^T P < 0 \tag{44}$$

where $\lambda_{min}(\Sigma)$ is the minimum eigenvalue of $\Sigma = H^T + H$.

When $c_2 \geq r_1$, the impact of the time-varying external disturbance $u_0(t)$ can be fully eliminated, and (44) can be reduced to:

$$A^T P + PA + PBB^T P - c_1 \lambda_{min}(\Sigma) PBB^T P < 0 \tag{45}$$

Remark 4.1. When $c_2 \geq r_1$, the impact of the time-varying external disturbance $u_0(t)$ can be fully eliminated. That means no matter what acceleration or deceleration operations the leading CAV performs, the following vehicles can track the trajectory of the leading CAV. However, from the view of practical applications, c_2 contains practical physical meaning, a larger value of c_2 indicates a larger maximum acceleration of the following RVs. Currently, most CAVs are electric vehicles, while RVs are usually fuel vehicles with less sensing capability, RVs are less reactive than CAVs. Thus, the control parameter $c_2 \geq r_1$ is not useful in some practical platoon systems. And in this case, ISSS shows its advantage of being able to describe the existence of bounded state under the bounded disturbance. From a more practical view, under the constraint $0 < c_2 < r_1$, ISSS has been proven to hold under Theorem 4.1 and Theorem 4.2 for the proposed control schemes in (11) under the CTH policy and CSH policy, respectively.

5. Numerical examples

This section verifies the effectiveness of the control schemes in (11) via numerical simulations under various scenarios. As mentioned, under the heterogeneous mixed traffic with CAVs and RVs, the leading vehicles (i.e., the CAVs) are used to guide the following vehicles (i.e., the RVs) while ensuring that the following RVs maintain the trajectories of the leading CAVs.

The dynamics of the vehicles are described by (5). Consider a single group of vehicles composed of one leading CAV and six following RVs in Example 5.1 and Example 5.2, and multiple groups of vehicles in Example 5.3. The leading vehicles are CAVs that are capable of self-navigation by following the trajectory optimized by the TMC. Because the CSH policy can be viewed as a special case of the CTH policy by letting $\tau = 0$ for all following RVs, this section focuses on the validation of Theorem 4.1. The control schemes in (11) are used to regulate the longitudinal motions and lateral motions of the following RVs, and the parameters of the proposed control schemes (11) c_1, c_2 and K are designed by solving the ISSS conditions (32) in Theorem 4.1.

Example 5.1. Straight road case for longitudinal control of a single platoon

Example 5.1 (a 1-dimensional straight road case for longitudinal control of a single platoon) is performed to validate the efficiency of the proposed vehicle platoon control scheme (11) while using CTH policy for a single platoon. In this example, all vehicles are assumed to be driving on a straight road, and the platoon control objective is to regulate the longitudinal positions and velocities of the following RVs such that the following RVs can track the longitudinal motion of the leading CAV.

The leading CAV receives information from the TMC through the V2I communication and executes the control commands. $\lfloor t \rfloor$ is a downward rounding function which rounds each element of the duration array t to the nearest number of seconds less than or equal to that element. In Example 5.1, the disturbance $\omega_i(t)$

is assumed to performed on $3th$ following RV (the middle of the platoon) by $\omega_3(t) = 3 \times (-1)^{\lfloor t \rfloor}$. In this example, the leading CAV is assumed to accelerate by the following three profiles:

- (a) The leading CAV drives by step-function signal, i.e., $u_0(t) = 3 \times (-1)^{\lfloor t/2 \rfloor}$.
- (b) The leading CAV drives by sinusoidal function signal, i.e, $u_0(t) = 3sin(2t)$.
- (c) The leading CAV drives by the following cruise mode:

$$u_0(t) = \begin{cases} 3 & 0 \le t < 5\ s, \\ 0 & 5 \le t < 10\ s, \\ -3 & 10 \le t < 15\ s, \\ 0 & 15 \le t < 20\ s, \end{cases} \tag{46}$$

Let $A = \begin{bmatrix} 0 & 1 \\ 0 & 0 \end{bmatrix}$, and $B = \begin{bmatrix} 0 \\ 1 \end{bmatrix}$. Then, (32) in Theorem 4.1 can be solved with appropriate value by $c_1 = 7$, $c_2 = 3$, and $P = \begin{bmatrix} 1 & 0 \\ 0 & 2 \end{bmatrix}$, $K = -(B+E)^T P = \begin{bmatrix} -1 & -2 \end{bmatrix}$. Then, the control scheme (11) can be applied to regulate the motion of the following RVs.

The desired longitudinal time headway of vehicle i is set to $\tau = 1$ s, and the desired intervehicular longitudinal standstill distance between two consecutive vehicles is assumed to be the same for all vehicles, i.e., $s_i = 5$ m for $i = 1, 2, \cdots, N$. The initial states of the vehicles are stated as Table 1.

Table 1: The Initial States of Platoon in Example 1

Platoon Index		Position (m)	Velocity (m/s)
String 1	the leading CAV	290	15
	the following RV 1	270	16
	the following RV 2	257	16
	the following RV 3	242	14
	the following RV 4	231	15
	the following RV 5	223	14
	the following RV 6	214	16

The simulation is performed under the control scheme in (11). Fig. 2 depicts the simulation results of Example 5.1. The longitudinal state trajectories of the leading CAV and the following RVs of three drive profiles are shown in Fig. 2(a),(c),(e), respectively. The longitudinal state trajectories of the following RVs converge to the longitudinal state of the leading CAV as demonstrated in Fig. 2(a),(c),(e).

And the norm of the state-tracking deviations of the following RVs of three drive profiles is shown in Fig. 2(b),(d),(f), respectively. According to the result of Fig. 2(b), (d), (f), the norm of the tracking deviations $x_i(t)$ between vehicle i and $i-1$ decrease along with the vehicle platoon, i.e., the perturbations are dissipated as they propagate along with the vehicles in the platoon. And Fig. 2(b), (d), (f) depicts the good performance of the state-tracking deviations of all following RVs that the norm of the state-tracking deviations remains bounded regardless of the existence of the unknown external control input of the leading CAV ($u_0(t)$) and

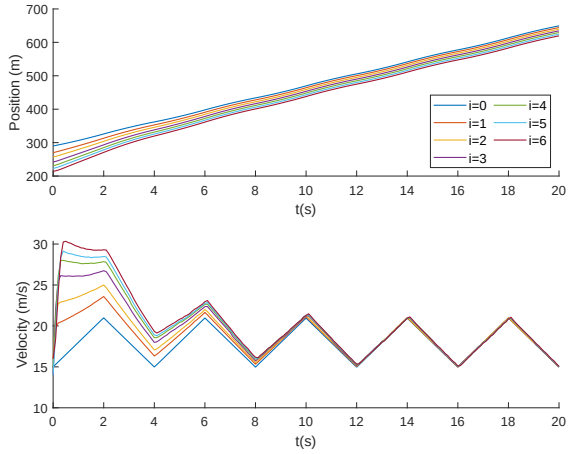

(a) State trajectories of the leading CAV and following RVs under step-function signal in Example 5.1

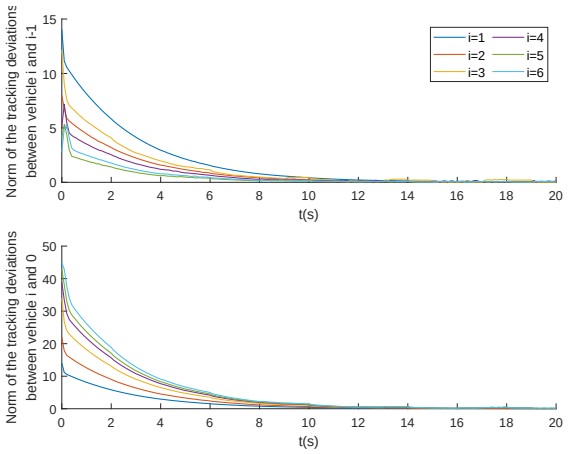

(b) Norm of the tracking deviations of the following RVs under step-function signal in Example 5.1

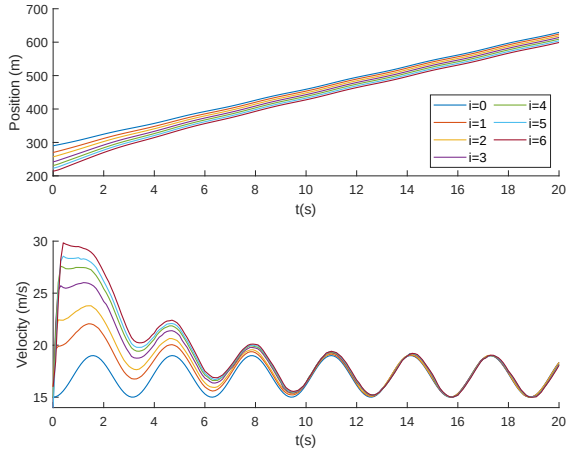

(c) State trajectories of the leading CAV and following RVs under sinusoidal function signal in Example 5.1

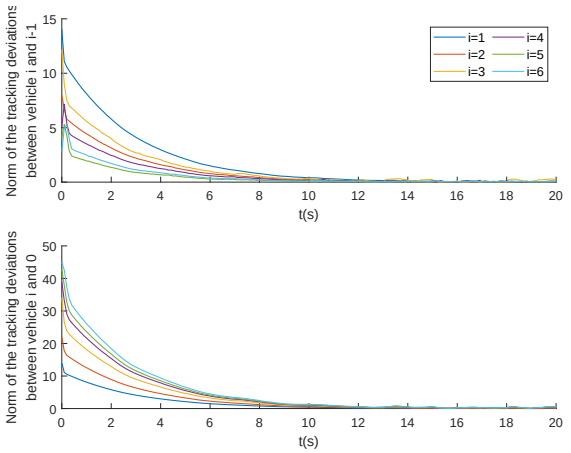

(d) Norm of the tracking deviations of the following RVs under sinusoidal function signal in Example 5.1

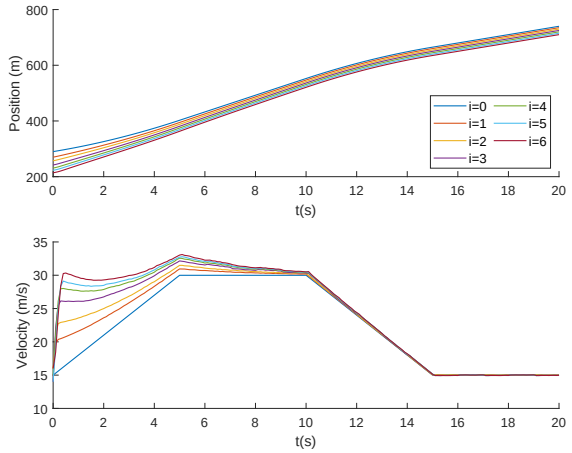

(e) State trajectories of the leading CAV and following RVs under cruise mode in Example 5.1

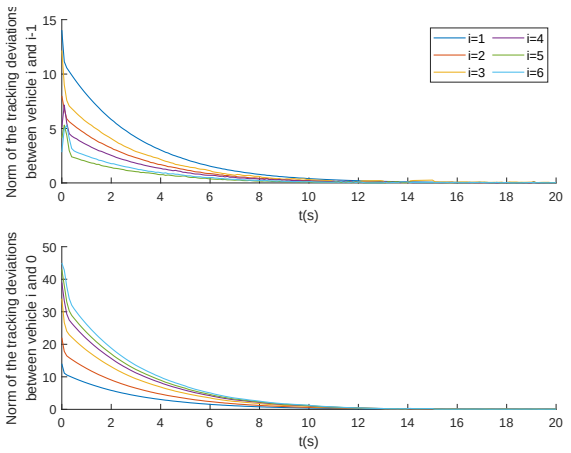

(f) Norm of the tracking deviations of the following RVs under cruise mode in Example 5.1

Fig. 2. Simulation results of Example 5.1

disturbances $\omega_i(t)$ (the uncertainty of the actuator via human drivers). Although the disturbances $\omega_i(t)$ are performed in the middle of the platoon, the performance of the platoon is still stable enough. From Fig. 2, we can see that once the platoon converges to be stable, the whole platoon will keep consensus, no matter how the leading CAV accelerates or decelerates with a bounded value.

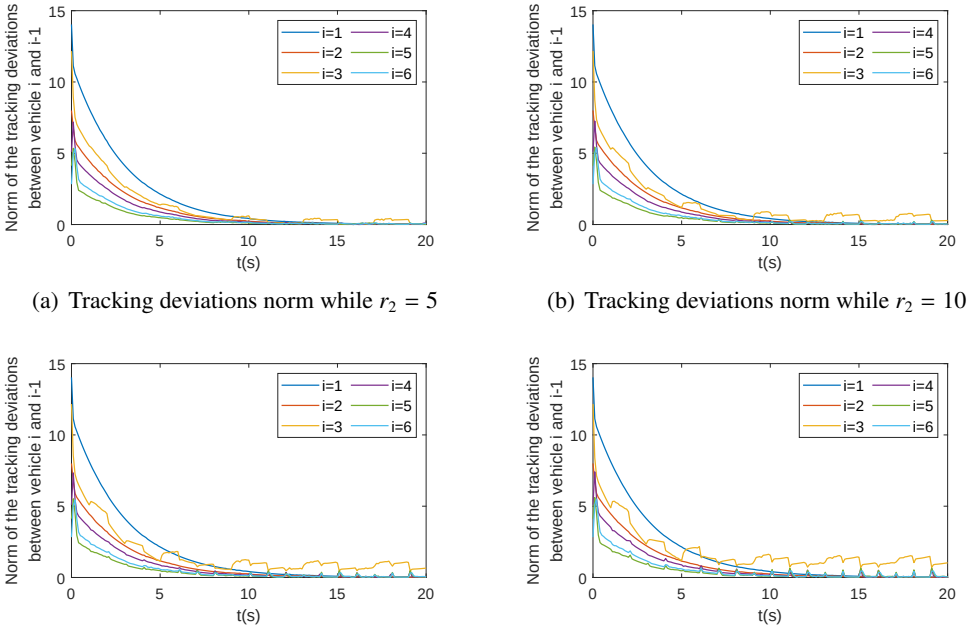

(a) Tracking deviations norm while $r_2 = 5$

(b) Tracking deviations norm while $r_2 = 10$

(c) Tracking deviations norm while $r_2 = 15$

(d) Tracking deviations norm while $r_2 = 20$

Fig. 3. Simulation results under different values of the disturbance $\omega_i(t)$

To analyze the influence of the value and position of the disturbance $\omega_i(t)$, sensitivity analysis of disturbance $\omega_i(t)$ is conducted. The disturbance $\omega_i(t)$ is assumed to performed on $3th$ following RV (the middle of the platoon) by $\omega_3(t) = r_2 \times (-1)^{\lfloor t \rfloor}$, where $r_2 = 5, 10, 15, 20$ respectively. From the result of the simulation, as shown in Fig. 3, the amplitude of the fluctuations increases with the increase of the upper bound of disturbance $\omega_i(t)$. However, the fluctuations are small on the whole and bounded even under unrealistically mild conditions (the external disturbance usually does not exceed 10).

To analyse the influence of the disturbance $\omega_i(t)$, the disturbance is set to perform on different vehicles, and the disturbance $\omega_2(t) = 3 \times (-1)^{\lfloor t \rfloor}$, $\omega_3(t) = 3 \times (-1)^{\lfloor t/2 \rfloor}$, $\omega_4(t) = 3 \times (-1)^{\lfloor t/4 \rfloor}$, $\omega_5(t) = 3 \times (-1)^{\lfloor t/5 \rfloor}$ are set to be active under corresponding scenarios. The result of the simulation is showed in Fig. 4. From Fig. 4, the influence of the position of disturbance is very tiny, the overall performance of the platoon does not decline much.

Thus, the objective is achieved by utilizing the proposed control schemes to bind the state deviations of the following RVs under bounded external disturbances and follow the leading CAV, i.e., the ISSS of the vehicle platoon is ensured. By using our proposed control schemes, the leading CAV can guide the travel of the following RVs to pass through the straight road according to Example 5.1.

Example 5.2. Curved road case for lateral and longitudinal control of a single platoon

As extensions of this practical application, Example 5.2 is performed to validate the efficiency of the

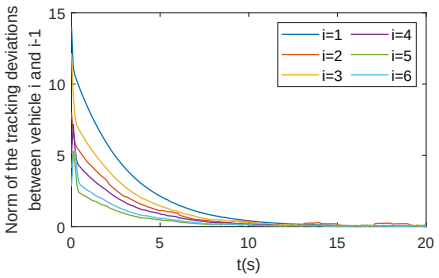

(a) Tracking deviations norm while the disturbance performed on vehicle 2

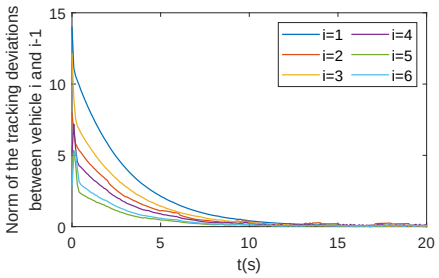

(b) Tracking deviations norm while the disturbance performed on vehicle 2 and 3

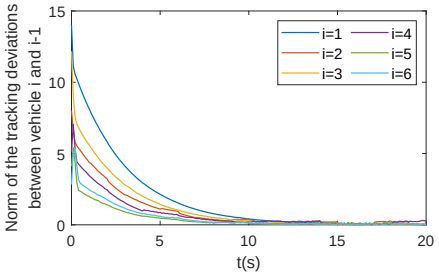

(c) Tracking deviations norm while the disturbance performed on vehicle 2, 3 and 4

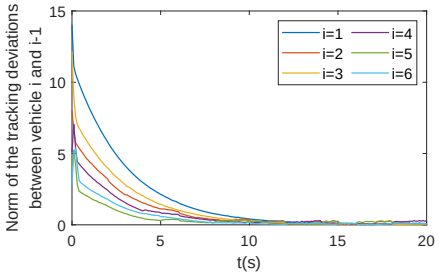

(d) Tracking deviations norm while the disturbance performed on vehicle 2, 3, 4 and 5

Fig. 4. Simulation results under different positions of the disturbance $\omega_i(t)$

proposed control schemes (11) for a single platoon (2-dimensional curved road case for longitudinal and lateral control). In this example, it is assumed that the leading CAV is driving with a time-varying velocity on a curved road, and the longitudinal and lateral positions and velocities of the following RVs need to be regulated. The initial states of the vehicles are stated as Table 2.

Table 2: The Initial States for Platoon in Example 5.2

Platoon Index		Position (m)	Velocity (m/s)
String 1	the leading CAV	(310,0)	(15,0)
	the following RV 1	(286,-1)	(16,0.5)
	the following RV 2	(264,1)	(16,-0.5)
	the following RV 3	(247,-1)	(14,0.5)
	the following RV 4	(224,1)	(15,-0.5)
	the following RV 5	(206,-1)	(14,0.5)
	the following RV 6	(181,1)	(16,-0.5)

Accordingly, for Example 5.2, the corresponding state $x_i(t) = [p_{xi}(t), p_{yi}(t), v_{xi}(t), v_{yi}(t)]^T$, where $p_{xi}(t)$ and $p_{yi}(t)$ represent the longitudinal and lateral positions of vehicle i, respectively, and $v_{xi}(t)$, $v_{yi}(t)$ are the longitudinal and lateral velocities of vehicle i, respectively.

And the leading CAV is driven by accelerating to pass through the curved road, after accepting the

optimized trajectory planned by the TMC:

$$u_{x0}(t) = u_{y0}(t) = \begin{cases} 3 & 0 \le t < 5\ s, \\ 0 & 5 \le t < 10\ s, \\ -3 & 10 \le t < 15\ s, \\ 0 & 15 \le t < 20\ s, \end{cases} \tag{47}$$

The control input $u_i(t) = [u_{xi}(t), u_{yi}(t)]^T$, the disturbance $\omega_i(t) = [\omega_{xi}(t), \omega_{yi}(t)]^T$, $A = \begin{bmatrix} 0 & 1 \\ 0 & 0 \end{bmatrix} \otimes I_2$, $B = D = \begin{bmatrix} 0 \\ 1 \end{bmatrix} \otimes I_2$, the disturbance is assumed to performed on the longitudinal and lateral dynamics of $3th$ following RV (the middle of the platoon) by $\omega_{x3}(t) = \omega_{y3}(t) = 3 \times -1^{\lfloor t \rfloor}$.

The simulation is performed under the control scheme in (11). The parameter of the proposed control schemes (11) can be calculated by solve the (32) in Theorem 4.1. Similarly to Example 5.1, we can get $c_1 = 7$, $c_2 = 3$, and $K = -B^T P = \begin{bmatrix} -1 & -2 \end{bmatrix} \otimes I_2$. Let $\tau = \begin{bmatrix} 1 & \\ & 0 \end{bmatrix}$ s, i.e., the longitudinal and lateral desired time headway of vehicles is 1 s and 0 s, respectively. Let $s_i = \begin{bmatrix} 5 & \\ & 0 \end{bmatrix}$ m, i.e., the longitudinal and lateral desired intervehicular standstill distance between two consecutive vehicles is 5 m and 0 m, respectively. And the values of the other parameters are the same as in Example 5.1

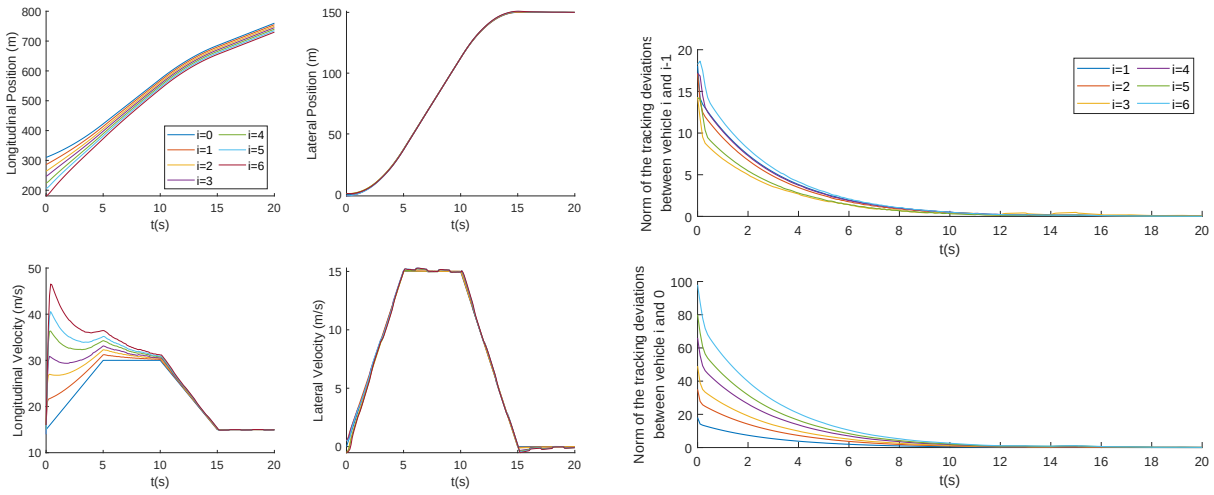

(a) State trajectories of the leading CAV and following RVs for the curved road in Example 5.2

(b) Norm of the tracking deviations of the following RVs for the curved road in Example 5.2

Fig. 5. Simulation results of Example 5.2

Then, we obtain the state trajectories of the leading CAV and following RVs shown in Fig. 5(a), and the norm of the tracking deviations shown in Fig. 5(b). The bounded unknown external control input of the

CAV (i.e., $u_0(t)$ that is regarded as disturbance) and bounded disturbances $\omega_i(t)$ generate bounded tracking deviations of vehicles. The state trajectories of the following RVs converge to the state of the leading CAV as demonstrated in Fig. 5(a), though there is some fluctuation under the influence of $\omega_i(t)$.

As $u_0(t)$ converges to zero, the norm of the tracking deviations of the following RVs converges to zero, as shown in Fig. 5(b). And all following RVs can drive with the desired inter-vehicular distance while maintaining the same velocities as those of the leading CAV when the leading CAV travels by a curved trajectory. As shown in Fig. 5(a), Fig. 5(b), the platoon is driven to form a stable formation under the external disturbances by utilizing our proposed control schemes, and the ISSS of the vehicle platoon is ensured. The leading CAV can guide the route of the following RVs to pass through the curved road according to Example 5.2.

Example 5.3. Straight road case for control of multiple platoons

In this example, as stated in Remark 2.1, the efficiency of (11) for multiple platoon control is validated. Three platoons (indexed by platoon $k = 1, 2, 3$, where platoon 1 is assumed to be the leading platoon), where each platoon is composed of 1 leading CAV and 6 following RVs, are considered in this simulation. It is assumed that 3 leading CAVs are driving with a time-varying velocity on a straight road and the following RVs follow the leading CAV of each platoon, all leading CAVs cooperate and drive in a constant formation. The optimized control demands of the leading CAVs of the leading platoon are transmitted from the TMC by the wireless network or planned by itself.

The cooperation of leading CAVs can also be considered as a platoon control mechanism, where the leading CAVs of other platoons are forced to follow the motion of the leading CAV of the leading platoon (platoon 1) while maintaining the desired state deviations. Use $\Delta d_0^k(t)$ and $\Delta v_0^k(t)$ to represent the position deviation and speed difference of the leading CAV of platoon k corresponding to the leading CAV of the leading platoon, respectively. Similar control schemes can be used to regulate the longitudinal and lateral motions of leading CAVs like in (11), i.e., the longitudinal control schemes and lateral control schemes for the leading CAVs in string k ($k = 1, 2, 3$) are designed as follows:

$$u_0^k(t) = c_1 K x_0^k(t) + c_2 g\left(x_0^k(t)\right) \tag{48}$$

where $u_0^k(t)$ represents the control input of the leading CAV of platoon k and $x_0^k(t) = [\Delta d_0^k(t), \Delta v_0^k(t)]^T$ represents the state-tracking deviations of the leading CAV of platoon k corresponding to the leading CAV of the leading platoon.

Use $\Delta d_i^k(t)$ and $\Delta v_i^k(t)$ to represent the position deviation and speed difference of the following RV i of platoon k corresponding to the following RV $i-1$ of platoon k, respectively. Then, the extension of (11) to the multiple platoons control scenario is used to regulate the following RVs:

$$u_i^k(t) = c_1 K x_i^k(t) + c_2 g\left(x_i^k(t)\right) \tag{49}$$

where $u_i^k(t)$ represents the control input of a following RV i of platoon k and $x_i^k(t) = [\Delta d_i^k(t), \Delta v_i^k(t)]^T$ represents the state-tracking deviations of the following RV i of platoon k corresponding to the following RV $i-1$ of platoon k. It can be seen from (49) that the control scheme of the following RVs of each platoon is the same as the single platoon control scheme (11). The initial states of the vehicles are stated as Table 3.

The leading CAV of string 1 is assumed to drive by:

$$\begin{aligned} u^1_{x0}(t) &= \begin{cases} 3 & 0 \le t < 5\ s, \\ 0 & 5 \le t < 10\ s, \\ -3 & 10 \le t < 15\ s, \\ 0 & 15 \le t < 20\ s, \end{cases} \\ u^1_{y0}(t) &= 0 \end{aligned} \tag{50}$$

The other settings are the same as in Example 5.2. Then, the position and velocity trajectories on the longitudinal and lateral dynamics of the leading CAVs and the following RVs of string 1, string 2, and string 3 are shown in Fig. 6(a), Fig. 6(b) andFig. 6(c), which show the trajectories of the following RVs converge to the trajectories of the leading CAV of the corresponding string, respectively. The norms of the state-tracking deviations of string 1, string 2, and string 3 can be obtained as shown in Fig. 6(d). As shown in Fig. 6(d), it is clear that the norms of the state-tracking deviations of all following RVs of string 1, string 2, and string 3 are bounded under external disturbances, and converge to zero at a very fast convergence rate.

From Fig. 6, we can see that the fluctuations occur in the lateral position and velocity profiles, this is the natural result of the disturbance $\omega_i(t)$, which is set to perform on 3th following RV (the middle of the platoon) of every platoon. It should be noted that the amplitude of the fluctuations is small, and the convergence rate is very fast. Especially, the vehicles can keep consensus even under the disturbance. The vehicles behind 3th following RV can keep the agreement with 3th following RV, and they all track the trajectory of the leading CAV, though fluctuations exist because of the influence of external disturbance.

The lateral positions and longitudinal positions of the leading CAVs and following RVs of the three platoons are shown in Fig. 7, where the red and black boxes represent the leading CAVs and the following RVs, respectively, and the set of colorful lines represent the trajectories of the leading CAVs and following RVs. The trajectory of all following RVs converge to the trajectory of the leading CAVs of the corresponding platoon, and the trajectory of the leading CAVs of string 2 and string 3 converge to the trajectory of the leading CAV of string 1 while maintaining the desired position deviations. Thus, the leading CAVs of string 1, string 2, and string 3 can guide the route of the following RVs to pass through the straight road according to Example 5.3. As shown in Fig. 6 and Fig. 7, all vehicles are driven to form a stable platoon formation even under the mild external disturbances by utilizing our proposed control schemes, and the ISSS of the vehicle platoon is ensured.

Table 3: The Initial States for Platoons in Example 5.3

Index		Position (m)	Velocity (m/s)	Desired gap (m)
String 1	the leading CAV	(310,0)	(15,0)	leading platoon
	the following RV 1	(286,-1)	(16,0.5)	
	the following RV 2	(264,1)	(16,-0.5)	
	the following RV 3	(247,-1)	(14,0.5)	
	the following RV 4	(224,1)	(15,-0.5)	
	the following RV 5	(206,-1)	(14,0.5)	
	the following RV 6	(181,1)	(16,-0.5)	
String 2	the leading CAV	(310,-10)	(15,0)	(0,10,0,0)
	the following RV 1	(286,-11)	(16,0.5)	
	the following RV 2	(264,-9)	(16,-0.5)	
	the following RV 3	(247,-11)	(14,0.5)	
	the following RV 4	(224,-9)	(15,-0.5)	
	the following RV 5	(206,-11)	(14,0.5)	
	the following RV 6	(181,-9)	(16,-0.5)	
String 3	the leading CAV	(310,10)	(15,0)	(0,-10,0,0)
	the following RV 1	(286,9)	(16,0.5)	
	the following RV 2	(264,11)	(16,-0.5)	
	the following RV 3	(247,9)	(14,0.5)	
	the following RV 4	(224,11)	(15,-0.5)	
	the following RV 5	(206,9)	(14,0.5)	
	the following RV 6	(181,11)	(16,-0.5)	

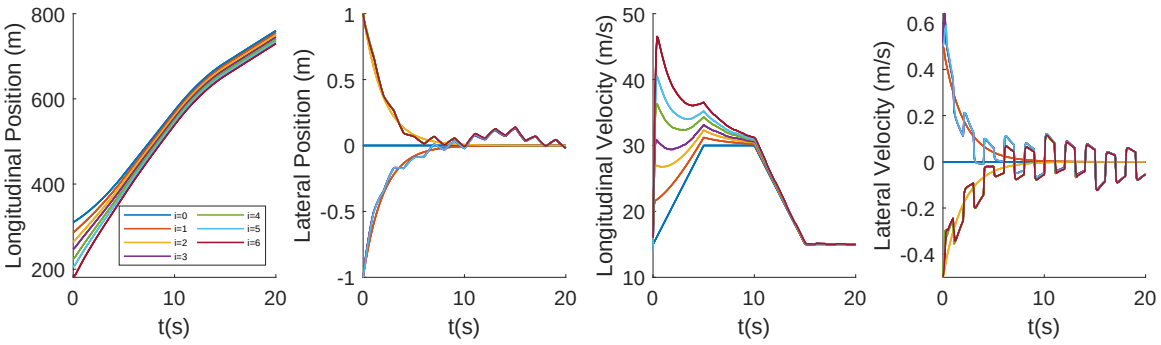

(a) Position and velocity trajectories on the longitudinal and lateral dynamics trajectories of string 1

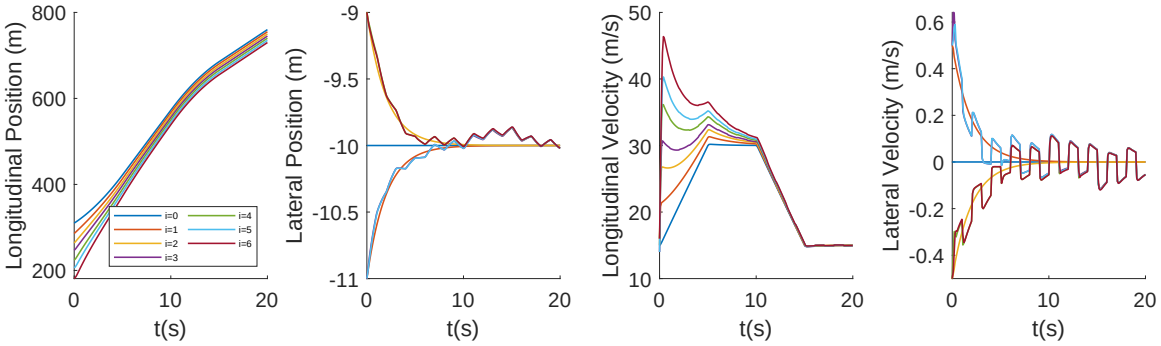

(b) Position and velocity trajectories on the longitudinal and lateral dynamics trajectories of string 2

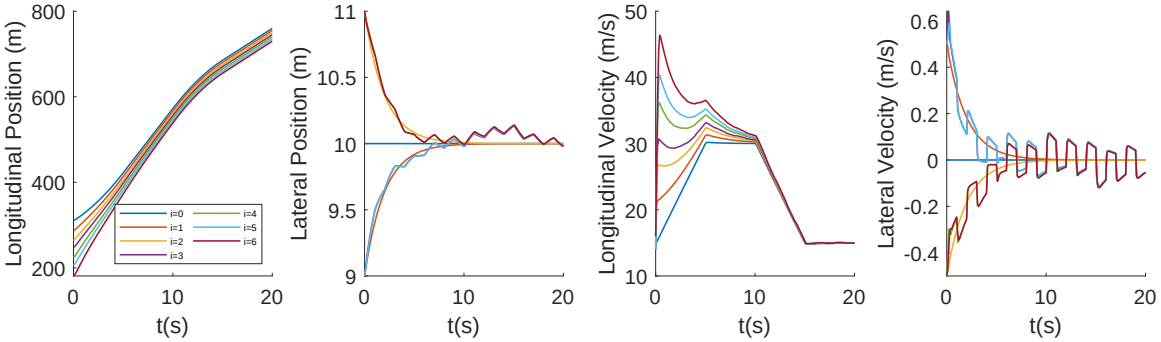

(c) Position and velocity trajectories on the longitudinal and lateral dynamics trajectories of string 3

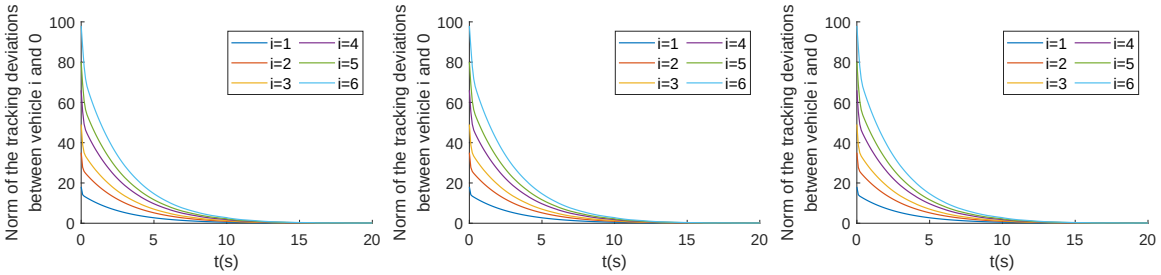

(d) Norm of the tracking deviations of string 1, 2 and 3

Fig. 6. Simulation results of strings 1, 2 and 3 in Example 5.3

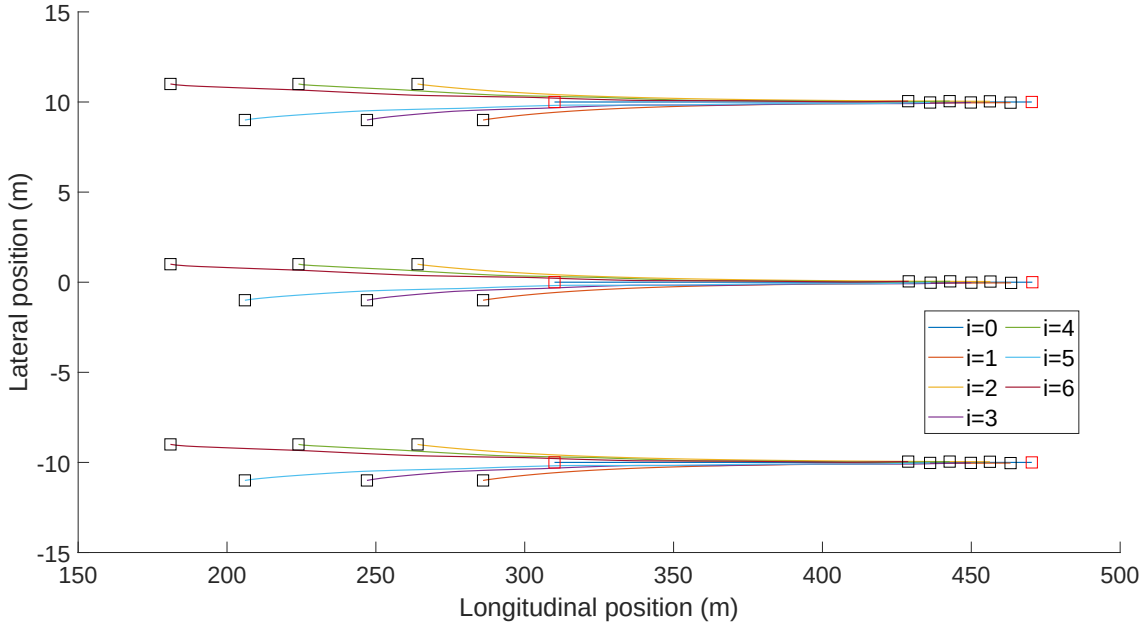

Fig. 7. Lateral positions and longitudinal positions of the leading CAV and following RVs of string 1, 2 and 3 in Example 5.3

6. Conclusions

In this paper, vehicular platoon control schemes stabilizing the mixed traffic flow of connected and automated vehicles (CAVs) and regular vehicles (RVs) were devised by using a CAV as the leading vehicle to guide the RVs in the platoon. Several practical challenges, such as the limited information perception capabilities of RVs, the uncertainty of actuators via human drivers, and external disturbances or unmodeled dynamics, were considered. Vehicular platoon control schemes under the constant space headway policy and constant time headway policy were synthesized through the lens of input-to-state-string stability (ISSS) while uncertainty and disturbance characteristics were considered. The control design utilized only the relative positions and velocities from the directly preceding vehicle, which could be sensed by the on-board sensors of commercially implemented adaptive cruise control (ACC) systems. Conditions for ISSS were derived while physical interpretations of these conditions were discussed. Furthermore, the relationships between ISSS and other state-of-the-art string stability concepts were clarified. It was concluded that the ISSS concept can include several state-of-the-art string stability concepts as special cases.

Corresponding to the longitudinal and lateral control schemes for a single platoon and multiple platoons, numerical experiments were performed. The norms of the tracking deviations and state trajectories of vehicles were plotted for the different examples, and all results showed that the platoon can effectively attenuate or reject the effect of disturbances while maintaining the ISSS property, the following RVs can adjust their accelerations to maintain the same velocities as those of the leading CAVs and the desired intervehicle distance by following the proposed platoon control schemes. Therefore, the leading CAVs can guide the motions of the following RVs. The results from numerical experiments validate the effectiveness and computational feasibility of the platoon control schemes.

7. Acknowledgments

The work described in this paper was jointly supported by the National Natural Science Foundation of China (72071214), National Key R&D Program of China (2018YFB1600500) and the Research Grants Council of the Hong Kong Special Administrative Region (Project No. PolyU R5029-18).

Appendix: preliminaries, useful lemmas and nomenclature

For a symmetric matrix A, $\lambda_{min}(A)$ and $\lambda_{max}(A)$ denote, respectively, its minimum and maximum eigenvalues. $A \otimes B$ denotes the Kronecker product of matrices A and B. $A > 0$ means that A is a positive definite matrix, and $A < 0$ means that A is a negative definite matrix.

We recall that a function $\alpha : [0, a) \to [0, \infty), a \in \mathbb{R}^+$ is a class $\mathcal{K}$ **function** if it is continuous, strictly increasing and $\alpha(0) = 0$. If a class $\mathcal{K}$ function α also satisfies $\alpha(s) \to \infty$ as $s \to \infty$, then it is a class $\mathcal{K}_\infty$ **function**. A continuous function $\gamma : [0, a) \times [0, \infty) \to [0, \infty)$ is a class $\mathcal{KL}$ **function** if for each fixed t, the function $\gamma(\cdot, t)$ is a class $\mathcal{K}$ function, and for each fixed s, $\gamma(s, \cdot)$ is decreasing and satisfies $\gamma(s, t) \to 0$ as $t \to \infty$.

For a vector $x \in \mathbb{R}^n$, $\|x\|$ denote its 2-norm, and $\|x\|_p$ denote its p-norm:

$$\|x\|_p = \left(\sum_{i=1}^{n} \|x_i\|^p \right)^{1/p}, p \in [1, \infty) \tag{51}$$

$$\|x\|_\infty = \max_i \|x_i\| \tag{52}$$

Given a Lebesgue measurable signal $x(t) : I \to \mathbb{R}^n$, $\|x\|_\infty^I$ denotes its $\mathcal{L}_\infty$ norm defined as $\|x\|_{\mathcal{L}_\infty}^I = \sup_{t \in I} \|x\|_\infty$, where the shorthand notation $\|x\|_\infty = \|x\|_\infty^{[0,\infty)}$ is used when $I = [0, \infty)$, and $\mathcal{L}_p$ norm of $x(t)$ is given as:

$$\|x\|_{\mathcal{L}_p}^I = \left(\int_I \|x(t)\|_p^p dt \right)^{1/p} < \infty, p \in [1, \infty) \tag{53}$$

Lemma 7.1. (Young's Inequality) (Bernstein, 2009) If a and b are nonnegative real numbers and θ and q are positive real numbers such that $\frac{1}{\theta} + \frac{1}{q} = 1$, then $ab \leq \frac{a^\theta}{\theta} + \frac{b^q}{q}$.

Table 4: Nomenclature

Notation	Type	Description	Notation	Type	Description
$x_i(t)$	vector	state of the ith vehicle	A/B	matrix	system matrices
$u_i(t)$	vector	control input of the ith vehicle	$\omega_i(t)$	vector	external disturbance of the ith vehicle
$u_0(t)$	vector	control input of the leading CAV from the TMC	r_1	vector	the acceleration bound of the leading CAV
$v_i(t)$	vector	the velocity of the ith vehicle	$p_i(t)$	vector	the position of the ith vehicle
$\mathcal{V}$	set	the set of the following vehicles	$\bar{\mathcal{V}}$	set	the set of the leading vehicle and the following vehicles
$\mathcal{L}$	matrix	the corresponding Laplace matrix of the sensing topology network	H	matrix	the link between the following vehicles and other following vehicles and the leading vehicle
$\mathcal{A}$	matrix	the adjacent matrix of graph of the following vehicles	$\mathcal{A}_0$	matrix	link between the following vehicles and leading vehicle
Σ	matrix	constructed positive definite matrix	P	matrix	positive definite solution to the matrix inequality
$d^*_{i,i-1}(t)$	vector	the desired intervehicular distance between two consecutive vehicles	$g(\cdot)$	vector	designed nonlinear function to eliminate the impact of $u_0(t)$
$\eta_i(t)$	vector	the tracking deviation from the desired state of vehicle i with respect to the leading CAV	$\eta(t)$	vector	the tracking deviation from the desired state of all vehicles with respect to the leading CAV
c_1/c_2	constant	designed constant gains of the platoon control schemes	u	vector	control input and disturbance vector of all vehicles
K	matrix	designed feedback gain matrix of the platoon control schemes	M	matrix	unitary matrix to transform Σ to diagonal matrix
s_i	vector	the desired standstill distance between vehicle i and vehicle $i-1$	τ	matrix	diagonal matrix that represents the desired time headway of vehicles
$\lambda_{min}(A)/$ $\lambda_{max}(A)$	operator	the minimum and maximum eigenvalues of a symmetric matrix A	$A \otimes B$	operator	the Kronecker product of matrices A and B
n	constant	the dimension of position $p_i(t)$ and velocity $v_i(t)$	$\mathbb{R}/\mathbb{N}$	set	real number set and natural number set

References

Bernstein, D. S., 2009. *Matrix mathematics: theory, facts, and formulas*. Princeton university press.

Besselink, B. and Johansson, K. H., 2017. String stability and a delay-based spacing policy for vehicle platoons subject to disturbances. *IEEE Trans. Autom. Control*, 62(9):4376–4391.

Bian, Y., Zheng, Y., Ren, W., Li, S. E., Wang, J., and Li, K., 2019. Reducing time headway for platooning of connected vehicles via v2v communication. *Transp. Res. Part C*, 102:87–105.

Cao, Y., Stuart, D., Ren, W., and Meng, Z., 2010. Distributed containment control for multiple autonomous vehicles with double-integrator dynamics: algorithms and experiments. *IEEE Transactions on Control Systems Technology*, 19(4):929–938.

Chen, D., Srivastava, A., Ahn, S., and Li, T., 2019. Traffic dynamics under speed disturbance in mixed traffic with automated and non-automated vehicles. *Transp. Res. Part C*, 133:293–313.

Eskandarian, A., Wu, C., and Sun, C., 2019. Research advances and challenges of autonomous and connected ground vehicles. *IEEE Trans. Intell. Transp. Syst.*, pages 1–29.

Feng, S., Zhang, Y., Li, S. E., Cao, Z., Liu, H. X., and Li, L., 2019. String stability for vehicular platoon control: Definitions and analysis methods. *Annu. Rev. Control*, 47:81–97.

Gunter, G., Gloudemans, D., Stern, R. E., McQuade, S., Bhadani, R., Bunting, M., Monache, M. L. D., Lysecky, R., Seibold, B., Sprinkle, J., Piccoli, B., and Work, D. B., 2020. Are commercially implemented adaptive cruise control systems string stable? *IEEE Trans. Intell. Transp. Syst.*, pages 1–12.

Jia, D. and Ngoduy, D., 2016. Platoon based cooperative driving model with consideration of realistic inter-vehicle communication. *Transp. Res. Part C*, 68:245–264.

Jia, D., Ngoduy, D., and Vu, H. L., 2019. A multiclass microscopic model for heterogeneous platoon with vehicle-to-vehicle communication. *Transp. Res. Part B*, 7(1):311–335.

Khalifa, A., Kermorgant, O., Dominguez, S., and Martinet, P., 2020. Platooning of car-like vehicles in urban environments: An observer-based approach considering actuator dynamics and time delays. *IEEE Trans. Intell. Transp. Syst.*, pages 1–13.

Konduri, S., Pagilla, P., and Darbha, S., 2017. Vehicle platooning with multiple vehicle look-ahead information. *IFAC-PapersOnLine*, 50(1):5768–5773.

Li, J., Ren, W., and Xu, S., 2011. Distributed containment control with multiple dynamic leaders for double-integrator dynamics using only position measurements. *IEEE Trans. Autom. Control*, 57(6):1553–1559.

Li, S. E., Zheng, Y., Li, K., and Wang, J., 2015. An overview of vehicular platoon control under the four-component framework. In *2015 IEEE Intelligent Vehicles Symposium (IV)*, pages 286–291. IEEE.

Li, Y., Tang, C., Li, K., He, X., Peeta, S., and Wang, Y., 2018. Consensus-based cooperative control for multi-platoon under the connected vehicles environment. *IEEE Trans. Intell. Transp. Syst.*, 20(6):2220–2229.

Li, Z., Liu, X., Ren, W., and Xie, L., 2012. Distributed tracking control for linear multiagent systems with a leader of bounded unknown input. *IEEE Trans. Autom. Control*, 58(2):518–523.

Liu, Y. and Su, H., 2019. Containment control of second-order multi-agent systems via intermittent sampled position data communication. *Appl. Math. Comput.*, 362:124522.

Lyashevskiy, S. and Meyer, A. U., 1995. Control system analysis and design upon the lyapunov method. In *Proceedings of 1995 American Control Conference-ACC'95*, 5:3219–3223. IEEE.

Monteil, J., Bouroche, M., and Leith, D. J., 2019. $\mathcal{L}_2$ and $\mathcal{L}_\infty$ stability analysis of heterogeneous traffic with application to parameter optimization for the control of automated vehicles. *IEEE Trans Control Syst Technol*, 27(3):934–949.

Pan, T., Lam, W. H., Sumalee, A., and Zhong, R., 2019. Multiclass multilane model for freeway traffic mixed with connected automated vehicles and regular human-piloted vehicles. *Transportmetrica A*, pages 1–29.

Pan, T., Guo, R., Lam, W. H., Zhong, R., Wang, W., and He, B., 2020. Integrated optimal control strategies for freeway traffic mixed with connected automated vehicles: A model-based reinforcement learning approach. *preprint*.

Peng, Z., Wang, D., Wang, H., and Wei, W., 2014. Cooperative iterative learning control of linear multi-agent systems with a dynamic leader under directed topologies. *Acta Automatica Sinica*, 40(11):2595–2601.

Ploeg, J., Van De Wouw, N., and Nijmeijer, H., 2013. Lp string stability of cascaded systems: Application to vehicle platooning. *IEEE Trans. Control Syst. Technol.*, 22(2):786–793.

Santini, S., Salvi, A., Valente, A. S., Pescapè, A., Segata, M., and Cigno, R. L., 2018. Platooning maneuvers in vehicular networks: A distributed and consensus-based approach. *IEEE Trans. Intell. Veh.*, 4(1):59–72.

Sontag, E. D., 2008. Input to state stability: Basic concepts and results. In *Nonlinear Optim. control theory*, pages 163–220. Springer.

Sontag, E. D. and Wang, Y., 1995. On characterizations of the input-to-state stability property. *Syst. Control. Lett.*, 24(5):351–360.

Stern, R. E., Cui, S., Delle Monache, M. L., Bhadani, R., Bunting, M., Churchill, M., Hamilton, N., Pohlmann, H., Wu, F., Piccoli, B., et al., 2018. Dissipation of stop-and-go waves via control of autonomous vehicles: Field experiments. *Transp. Res. Part C*, 89:205–221.

Talebpour, A. and Mahmassani, H. S., 2016. Influence of connected and autonomous vehicles on traffic flow stability and throughput. *Transp. Res. Part C*, 71:143–163.

Wang, C., Gong, S., Zhou, A., Li, T., and Peeta, S., 2020a. Cooperative adaptive cruise control for connected autonomous vehicles by factoring communication-related constraints. *Transportation Research Part C: Emerging Technologies*, 113:124–145.

Wang, S., Jiang, S., Zhan, Z., Wu, Y., and Zhong, R., 2020b. Output containment control of discrete-time multi-agent systems with application to multiple ground vehicles. *arXiv preprint arXiv:2005.11692*.

Wang, S., Zhan, Z., Zhong, R., Wu, Y., and Zhouhua, P., 2020c. Adaptive distributed observer design for containment control of heterogeneous discrete-time swarm systems. *Chinese Journal of Aeronautics*.

Wang, Z., Bian, Y., Shladover, S. E., Wu, G., Li, S. E., and Barth, M. J., 2020. A survey on cooperative longitudinal motion control of multiple connected and automated vehicles. *IEEE Trans. Intell. Transp. Syst.*, 12(1):4–24.

Xiao, L. and Gao, F., 2011. Practical string stability of platoon of adaptive cruise control vehicles. *IEEE Trans. Intell. Transp. Syst.*, 12(4):1184–1194.

Xie, D., Zhao, X., and He, Z., 2018. Heterogeneous traffic mixing regular and connected vehicles: Modeling and stabilization. *IEEE Trans. Intell. Transp. Syst.*, 20(6):2060–2071.

Zegers, J. C., Semsar-Kazerooni, E., Ploeg, J., van de Wouw, N., and Nijmeijer, H., 2017. Consensus control for vehicular platooning with velocity constraints. *IEEE Trans. Control Syst. Technol.*, 26(5):1592–1605.

Zhang, L. and Orosz, G., 2017. Consensus and disturbance attenuation in multi-agent chains with nonlinear control and time delays. *International Journal of Robust and Nonlinear Control*, 27(5):781–803.

Zhou, Y., Wang, M., and Ahn, S., 2019. Distributed model predictive control approach for cooperative car-following with guaranteed local and string stability. *Transp. Res. Part B*, 128:69–86.

Zhou, Y., Ahn, S., Wang, M., and Hoogendoorn, S., 2020. Stabilizing mixed vehicular platoons with connected automated vehicles: An h-infinity approach. *Transp. Res. Part B*, 132:152–170.